JOURNAL OF RAMAN SPECTROSCOPY
J. Raman Spectrosc. **31**, 863–870 (2000)

Valence band of liquid water Raman scattering: some peculiarities and applications in the diagnostics of water media

T. A. Dolenko, I. V. Churina, V. V. Fadeev* and S. M. Glushkov
Chair for Quantum RadioPhysics, Physical Department, Moscow State University, Moscow 119899, Russia

A short analysis of the results of our research on peculiarities of water Raman scattering spectra and of their applications in the diagnostics of water media is presented. The results of using a new approach for research on water Raman scattering spectra, i.e. the method of artificial neural networks for spectra treatment and for the solution of inverse problems in water media diagnostics, are also presented. This technique allowed us to improve the accuracy of water temperature determination (error 0.3 °C) by exploiting the temperature dependence of valence band parameters. However, no peculiarities of this dependence in the vicinity of 20, 36 and 76 °C, reported by others, were discovered.

INTRODUCTION

In the 1980s, there was increasing interest in research on the Raman scattering valence band of liquid water. The following problems were considered:

1. Investigation of the peculiarities in the behavior of the Raman scattering valence band of water under the influence of different factors (temperature, pollutants present, pressure, geometric factors of spectral curves of excitation and recording, etc.).
2. The use of results of such research for the verification of liquid water structure models, and search for peculiarities in the behavior of that band, connected with anomalous water properties.
3. The use of the Raman scattering band in laser diagnostics of water media in three directions:
   - the use of the Raman scattering band as an internal benchmark, and therefore a study of its intensity versus media factors (i.e. a study of the internal benchmark stability);
   - measurement of water temperature and salinity;
   - determination of parameters of heterophase systems containing water in solid and liquid phases, and the use of polarization peculiarities of the water Raman band to study the water crystallisation process.

By the end of the 1980s, the possibilities in research on the valence Raman scattering band had been exhausted. The revealed regularities in the behavior of Raman scattering spectra under the influence of different factors did not allow one to choose any particular model of the water structure. These regularities did not give an explanation of the well-known anomalous water properties and did not discover new properties. When the Raman scattering band was used to determine water temperature and salinity, the measurement accuracy of these parameters was 0.5 °C and 0.5‰, respectively, in cases when the water attenuation index dispersion could be taken into account.

In the last 2–3 years, new circumstances arose which stimulated resumption of research on water Raman scattering spectra peculiarities and of their application in water media diagnostics (in particular, in our laboratory):

1. Bunkin and Pershin[1,2] reported that in investigations of the temperature dependence of the water valence band Raman scattering they discovered anomalous peculiarities in the vicinity of 0, 4, 20, 36 and 76 °C. This interesting result attracted our attention since, as far as we know, such anomalies have never been observed before (including in our laboratory).
2. The development in recent years of a new method of spectra processing based on artificial neural networks. This method can provide major progress in the solution of the problems of the verification of water structure models and of water media diagnostics.

In this context, our group has resumed the investigation of the liquid water Raman scattering valence band. In this paper, we give a short review of the results of our research on water Raman scattering spectra peculiarities and of their applications in the diagnostics of water media, which had been obtained previously in our laboratory. We consider it appropriate to do so in this issue in dedicated to N. I. Koroteev, who displayed a keen interest in our work in this field. Further, this paper presents the results of the use of a new approach to studies of water Raman scattering spectra, namely the method of artificial neural networks for spectra treatment and for the solution of inverse problems in water media diagnostics.

INVESTIGATION OF TEMPERATURE DEPENDENCE OF WATER RAMAN SCATTERING VALENCE BAND

There are many published experimental data on the temperature dependence of the water Raman scattering

* Correspondence to: V. V. Fadeev, Chair for Quantum RadioPhysics, Physical Department, Moscow State University, Moscow 119899, Russia; e-mail: tdolenko@pop.radio-msu.net

Received 19 February 2000
Accepted 15 June 2000

spectrum valence band[1–21] and of water infrared spectra,[22–24] on the temperature dependence of water pair correlation functions[25–27] and on other characteristics of liquid water.

Our group has been investigating the dependence of the shape of the Raman scattering valence band on temperature since the 1980s.[10–16] During this period, a large amount of data in different temperature regions and under different experimental conditions (using different excitation sources and spectral analyzers) has been obtained.

The Raman scattering valence band of liquid water was studied in our laboratory in the temperature range 20–350 °C (an optical autoclave was used). These spectra were recorded with excitation with radiation of 488 nm from an argon ion laser, and with the help of parallel recording of spectra with an optical multi-channel analyzer (OMA). Typical spectra obtained in the high-temperature experiments (Fig. 1), and those obtained in the temperature range from −8 to 20 °C (in an optical cryostat[15]) repeat the temperature dependence of the water Raman scattering valence band observed by many other workers:[1–21] with the increase in temperature, the intensity of the low-wavenumber region decreases and that of the high-wavenumber region increases. When the temperature exceeds 150 °C, the low-wavenumber shoulder disappears completely. One can also note other peculiarities of the behavior of the Raman scattering band with increase in temperature from 20 to 350 °C (Fig. 1):

- in the spectra obtained, no isosbestic point was observed (in contrast to some studies[3,4] but and in accordance with others[1,2,5,10–14]);
- the wavenumber of the band maximum increases linearly with increase in temperature (Fig. 2);
- with increase in temperature, the width of the band decreases; the effect is most pronounced in the temperature range 120–180 °C, when the intensity of the low-wavenumber shoulder becomes less than half of that of the high-wavenumber shoulder;
- the area under the Raman scattering curve decreases with increase in temperature (Fig. 3).

We have carried out more accurate investigations of the behavior of the Raman scattering valence band in the temperature range 20–90 °C.[10–14] To describe the change in the Raman scattering valence band quantitatively, we

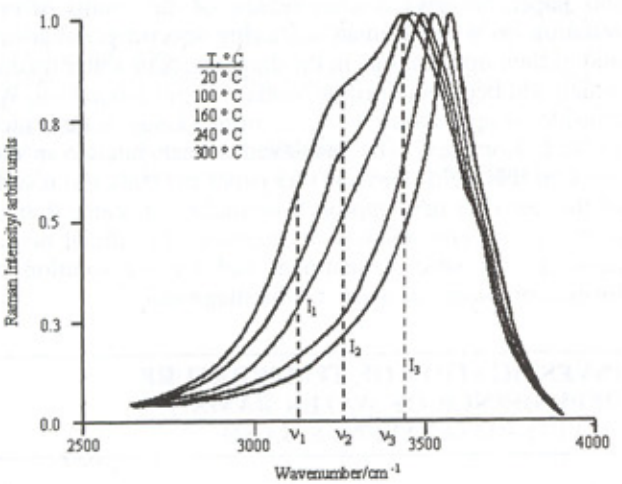

Figure 1. Raman spectra of liquid water at different temperatures.

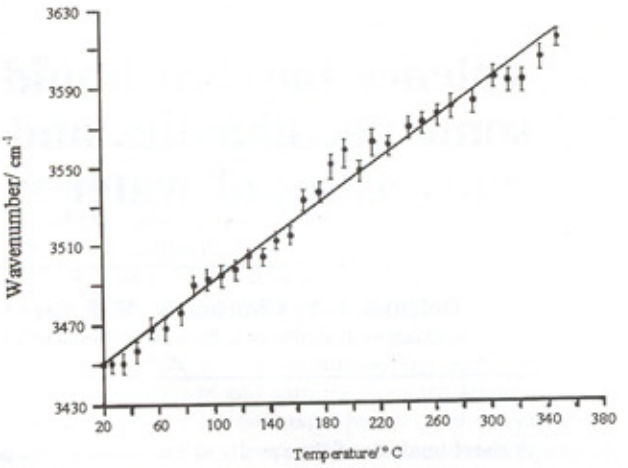

Figure 2. Maximum position of the Raman valence band of liquid water as a function of temperature *T*.

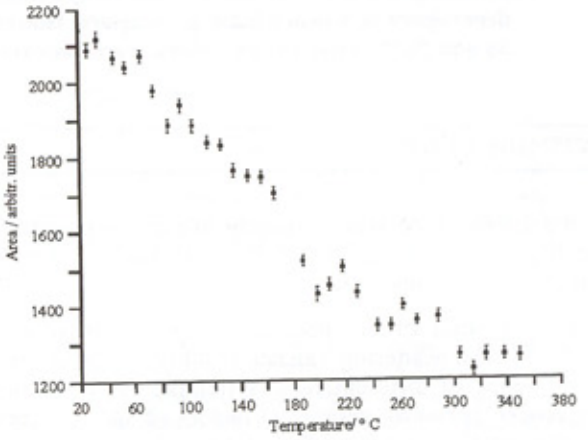

Figure 3. Dependence of the area *S* under the Raman valence band of liquid water on temperature *T*.

used the parameters χ_{31} and χ_{32}, namely the ratios of Raman scattering intensities at typical points of this band (Fig. 1). In the temperature range 20–90 °C, the dependences $\chi_{31}(T)$ and $\chi_{32}(T)$ were found to be linear (Fig. 4). These dependences can be used for the remote measurement of water temperature and of dissolved salt concentration (see the next section).

Figure 5 illustrates the change in the Raman scattering band of liquid water with the water being cooled to a supercooled state (in our experiments, down to −8 °C[15]).

The polarization properties of the water Raman band are also peculiar (see, for example, Refs 15–20). We cannot deal with them in detail within this paper (Ref. 20). We shall only note that the considerable difference between the spectral shapes of the polarized and depolarized components of the water Raman band opens up great opportunities in the diagnostics of water, in particular in its solid phase.

Figure 6 shows the Raman band shape for polycrystalline ice I_h as a function of the angle θ between the wavevector of the scattered radiation and the electric field vector of linearly polarized laser radiation entering the sample. As can be seen, these functions are substantially different in the cases when laser radiation propagates parallel to the direction of the temperature gradient taking place during crystallization, and perpendicular to this direction. We have explained this phenomenon earlier,[15,16] where we drew the

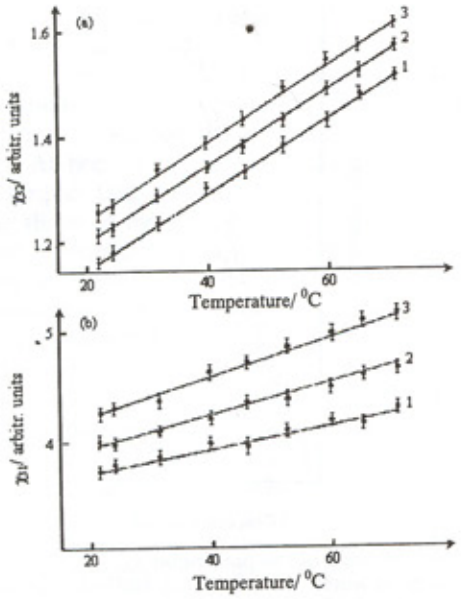

Figure 4. Temperature dependences of the parameters (a) χ_{32} and (b) χ_{31} for distilled water (1, salinity $S = 0$), for 'normal' sea water (3, $S = 35\%$) and for their mixture in 1 : 1 proportions (2, $S = 17.5‰$).

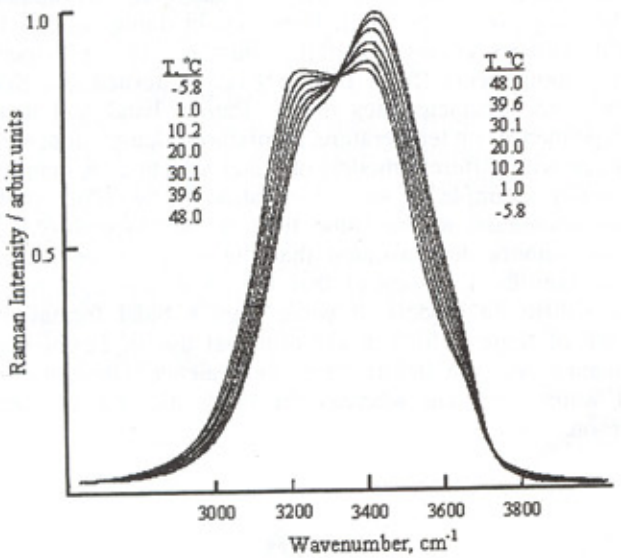

Figure 5. Dependence of the Raman valence band of liquid water on temperature T. Spectra normalized to unit area.

conclusion that differences in the Raman band behavior in cases (a) and (b) meant primary orientation of the crystal optical axis with the creation of polycrystalline ice along the direction of the temperature gradient. The behavior of Raman bands of the heterophase water system in the process of water crystallization[20] are even more interesting and in some cases seem 'anomalous.'

STUDY OF WATER RAMAN SCATTERING SPECTRA IN WATER SOLUTIONS OF ELECTROLYTES

Our subjects for study were water solutions of alkali metal halide salts with cations Li^+, Na^+, K^+, NH_4^+, and anions F^-, Cl^-, Br^-, I^- in the following concentration ranges:

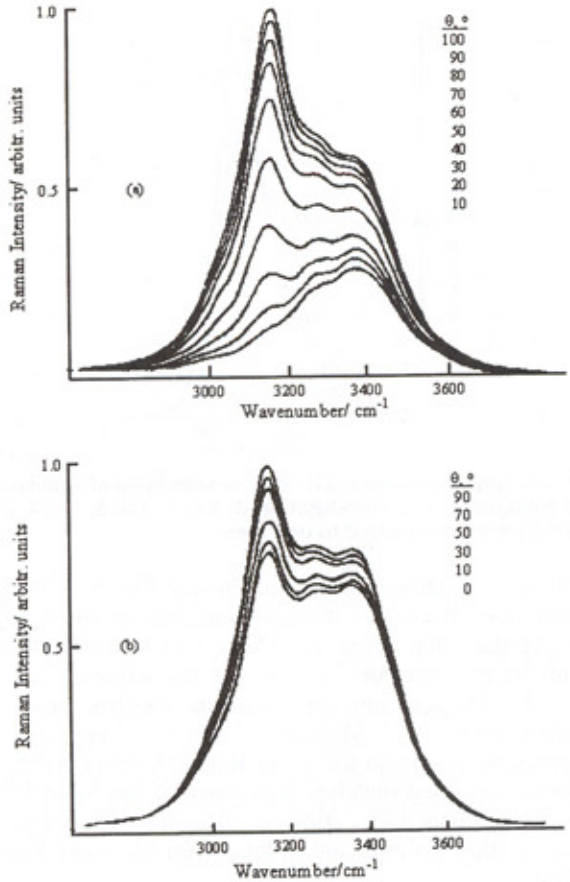

Figure 6. Dependence of the shape of Raman spectrum of polycrystalline ice I_h on angle θ between the wavevectors of the scattered and the incident radiation: for the direction of the exciting beam propagation (a) parallel to the direction of temperature gradient and (b) perpendicular to the direction of temperature gradient.

LiF 0.05–0.1, NaF 0.1–1.0, NH_4F 0.5–2.2, LiCl 0.5–19.6, NaCl 0.6–6.1, KCl 0.5–4.6, NH_4Cl 0.5–7.3, LiBr 0.5–10.0, NaBr 0.5–8.8, KBr 0.5–5.5, LiI 0.5–10.0, NaI 0.5–10.0 and KI 0.5–8.7 M.

The Raman scattering signal was excited by radiation from an argon ion laser with a wavelength of 514.5 nm. The Raman scattering spectra of water in the solutions were recorded at room temperature.

The experimental data obtained showed that with increasing concentration of ions dissolved in water, the intensity of the high-wavenumber spectrum region increases and that of the low-wavenumber region decreases; the band shifts to higher wavenumbers, and the bandwidth decreases (Fig. 7). An exception is the behavior of water Raman scattering spectra of the solutions of ammonium and fluoride salts.

Figure 8(a) shows the behavior of the water Raman spectra in solutions with the same concentration of the salt with different anions and the same cation, K^+, and Fig. 8(b) with different cations and the same anion, Cl^-.

Comparative analysis of the data obtained confirms that the intensity of water Raman spectra in solutions depends not only on the concentration C of the dissolved ions, but also on their type. This effect is demonstrated in Fig. 9 in the form of the $\chi_{32}(C)$ dependence. As can be seen, in the concentration range 0.5–4.0 M the $\chi_{32}(C)$ dependence can be approximated by a straight line for all the salts.

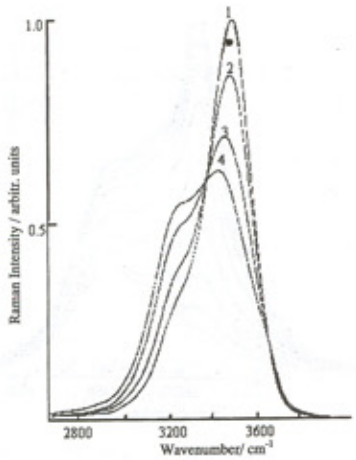

Figure 7. Dependence of the Raman valence band of liquid water in KI solution on salt concentration: 1, 5 M; 2, 3 M; 3, 1 M; 4, pure water. Spectra normalized to unit area.

The investigations carried out showed that the influence of anions on the water Raman band appears to be much stronger than that of cations. Note that the influence of anions on the spectrum increases in the sequence: $Cl^- < Br^- < I^-$. These results agree with the spectroscopic data of other workers.[28,29] Moreover, from the strength of the influence of anions on the water Raman valence band, the sequence obtained matches the theory of ion hydration.[30] A similar sequence for cations is difficult to obtain exactly owing to their insignificant influence on the water Raman spectra.

The abnormal behavior of the water Raman spectra in solutions of ammonium and fluoride salts can be accounted for by the individual properties of these ions.[14]

STUDY OF LIQUID WATER STRUCTURE USING PECULIARITIES OF RAMAN VALENCE BAND

A number of hypotheses trying to explain the structure of liquid water and its manifestations in Raman spectra have been proposed.[3–5,24–27] Attempts were made to decompose the contour of the water Raman valence band into components of different shapes (Gaussian, Lorentzian, their superpositions, etc.). However, in doing so, different workers obtained different numbers of such spectral components (from two to five). It turned out that the same characteristics of the Raman band and their dependences on temperature, admixtures, deuteration, etc., agree with different models of water structure. A demonstrative example of such a situation is two PhD studies completed at the same time in our laboratory.[15,21] The authors demonstrated that the experimental material (similar in essence) that they had collected fitted two different models of water Raman band formation. One of these models made principal use of Fermi resonance between deformation and valence vibrations in a water molecule whereas the other did not use this resonance.

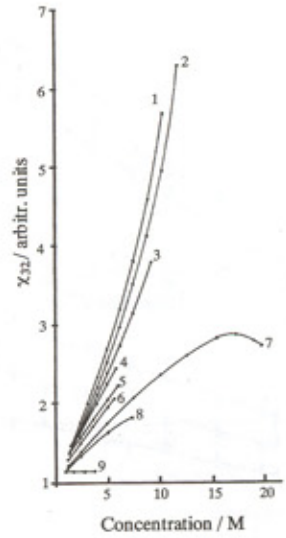

Figure 9. Dependence of the parameter χ_{32} on concentration of salts dissolved in water: 1, KI; 2, NaI; 3, NaBr; 4, KBr; 5, NaCl; 6, KCl; 7, LiCl; 8, NH_4Cl; 9, NH_4F.

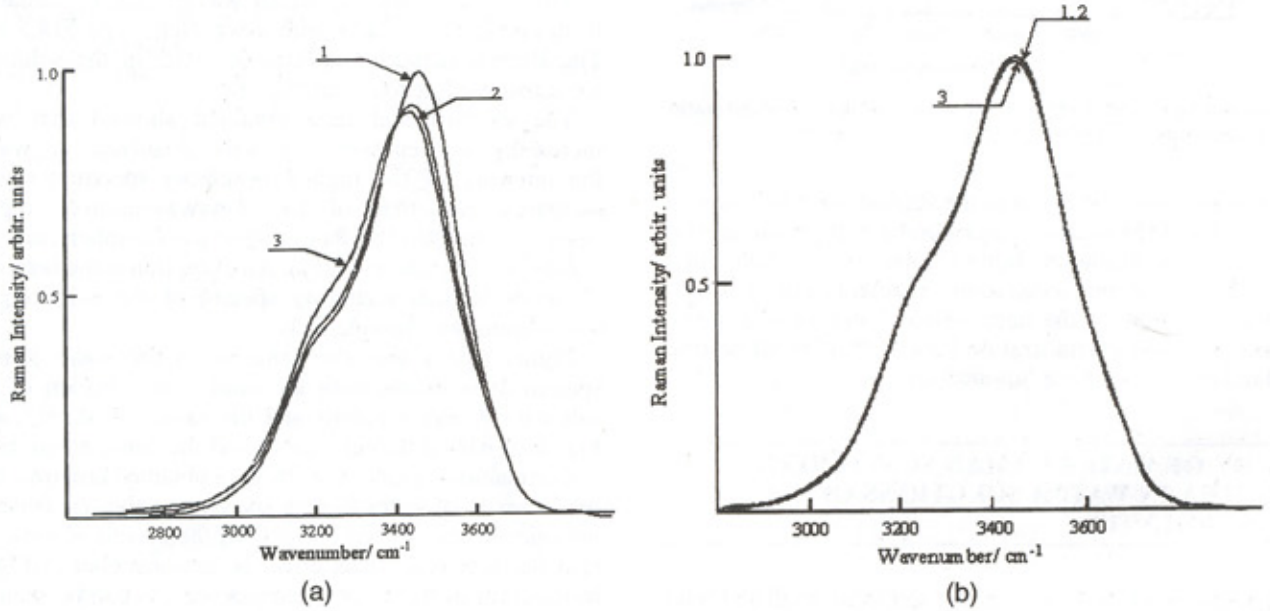

Figure 8. (a) Raman spectra of liquid water in solutions of potassium salts: 1, KI; 2, KBr; 3, KCl. Solution concentration 4 M. (b) Raman spectra of liquid water in solutions of chloride salts: 1, LiCl; 2, KCl; 3, NaCl. Solution concentration 4 M.

The reason for such ambiguities lies in the fact that the models contain many fitting parameters, and that the variation methods of analysis generally used cannot provide uniqueness of the solution. Here we applied a new approach based on the method of artificial neural networks. At present we are exploiting this approach to solve a simpler task of water temperature determination using the shape of the Raman band (see later).

A great contribution to the study of liquid water structure could be made by the discovery of some peculiarities in the temperature dependences of the characteristics of water Raman bands in the points of the known anomalies of liquid water properties, especially at the temperatures 0 °C (water–ice phase transition), 4 °C (maximum density) and 36 °C (minimum isobaric heat capacity).

Numerous experiments carried out by our group and briefly summarized above did not reveal any peculiarities at the listed temperatures. Peculiarities also had not been noted in the publications of other workers either, up to the publication of the papers by Bunkin and Pershin,[1,2] which for the above reasons were noted with interest.

Bunkin and Pershin recorded experimental Raman spectra of water in the temperature range −6 to +80 °C. During the spectral processing, fitting by the least-squares method was used to approximate the band contour by the Gaussian and Lorentzian curves. Observing a temperature deformation of the Raman band contour, the authors considered that temperature changes in the statistical weight of the right and left parts of the spectrum should manifest themselves in the temperature shift of the center of the approximating envelope. Then position of the center of the Lorentzian and Gaussian envelopes, approximating the experimental spectra, as a function of temperature is presented (λ_{exc} = 532 nm) in Fig. 10(a). It was noticed that with increase in temperature, the position of the center shifted monotonically towards higher wavenumbers. However, along with the monotonic shift, there are sharp deviations from the mean value, exceeding the value of the spread of the experimental results in the temperature regions of about 4, 20, 36 and 76 °C. Of these four values, two (4 and 36 °C) are well known as the temperature of maximum water density and the temperature of the minimum value of its isobaric heat capacity, respectively. The other two are less well known and mark the regions of maximum surface tension and of maximum speed of sound. Such a correlation of the discovered peculiarities with extreme values of water macro-parameters stimulated additional experiments to be performed in the temperature range from −6 to +80 °C with the determination of the width of the envelope.

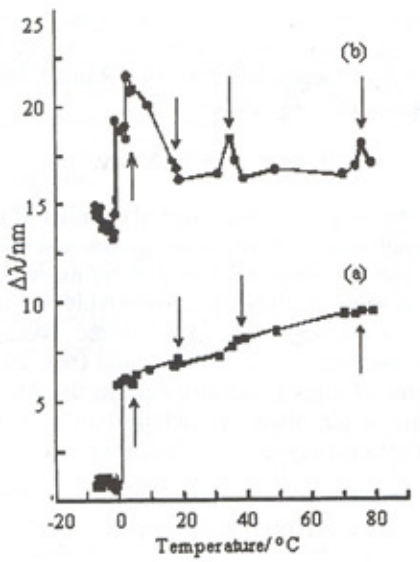

Figure 10. Temperature dependence of the shift of (a) the envelope center and (b) the envelope width for Gaussian envelope of the Raman valence band of water[2] (λ_{exc} = 532 nm).

It turned out that the width of the spectrum envelope at the listed temperature points suffered abrupt changes [Fig. 10(b)], broadening (~2 nm) in the vicinity of these critical temperatures of 4, 16, 36 and 76 °C. Such anomalies were observed in the water Raman spectroscopy for the first time.

Having studied the two publications,[1,2] we thoroughly re-checked our results obtained before and processed them according to the procedure described by Bunkin and Pershin.[1,2] Unfortunately, we obtained no confirmation of their conclusions. We did not observe any peculiarities when processing the spectra by the method of artificial neural networks (ANN) either.

We consider that the reason for this discrepancy lies in the insufficient precision of their measurements and also in our experiments. Since the question under consideration is extremely important for the whole problem of the Raman spectroscopy of water, we intend to perform a more thorough search for the peculiarities, improving the precision of measurements, especially in the vicinity of the mentioned 'special points,' and using several methods of data processing simultaneously, including both the method used by Bunkin and Pershin[1,2] and the method of ANN used by us.

WATER RAMAN BAND AS AN INTERNAL BENCHMARK IN WATER MEDIA FLUORIMETRY

The method of the internal benchmark, i.e. continuous calibration of the fluorescence band intensities (the number of photons) of organic admixtures in water to the intensity of the simultaneously recorded water Raman band, was substantiated[8,9,31] and first applied under natural conditions[32] over 20 years ago.

The key question here is the stability of the water Raman band intensity under the experimental conditions. If the temperature range is limited to 0–30 °C and the salinity range is limited to 0–40‰, then the intensity (or the number of photons) of the Raman band does not change more than by a few per cent. For sea water, the concentration of the main organic components (aquatic humic substance, phytoplankton pigments, protein compounds, oil pollutants, etc.) is such that the intensities of their fluorescence bands usually do not exceed the intensity of the water Raman band, i.e. the parameter $\Phi_0 = N_{fl}/N_{RS} \leq 1$ (N is the number of emitted photons). In this case, the influence of such organic compounds on the intensity of the water Raman band is also insignificant.

In some situations (e.g. inland water basins), the parameter for the aquatic humic substance Φ_0^{AHS} may increase up to values of about 20, which leads to a nearly 15% decrease in the intensity of the water Raman band.

DETERMINATION OF TEMPERATURE AND SALINITY OF SEA WATER BY LASER RAMAN SCATTERING SPECTROSCOPY

At the present stage of its development, oceanology urgently needs the elaboration of express and remote methods of determination of sea water parameters, in particular, methods for the determination of water temperature and salinity. Measurements of the above parameters are of considerable importance since they are widely used in the study of water mass dynamics and in water ecosystems monitoring. To obtain information about the parameters of the sea water media, remote laser sensing methods based on the spectral analysis of echo signals[8–16] are now widely used.

Experimental investigations of the temperature dependence of the water Raman scattering curve (see earlier) showed that with a change in temperature, the shape of the Raman scattering valence band also varied. Although these changes are small, they are readily detectable by modern measurement methods. Quantitatively these changes were described with the parameters $\chi_{31}(T)$ and $\chi_{32}(T)$ (Fig. 1). Using the linear section of the dependence $\chi_{32}(T)$, Leonard and co-workers[8,9] developed and tested a method for measuring the temperature of water media with an accuracy of 0.5 °C in laboratory conditions and 2 °C in natural conditions.

It follows from other studies[28,29] and from our results, obtained not only for the solutions of electrolytes but also for 'normal' sea water (salinity 35‰) at different levels of dilution with distillate in laboratory experiments,[10–14] that the shape of the water Raman band depends also on the admixtures present in the water. Therefore, when measuring the sea water temperature with the help of Raman spectroscopy, it is necessary to take into account the influence of the salts present on the shape of the Raman spectrum.

'Three-wavenumber' method of simultaneous determination of water temperature and salinity from Raman spectra

It has been shown[12,14] that from the shape of the water Raman band it is possible to determine both sea water parameters, i.e. temperature T and salinity S, simultaneously. In principle, the possibility of simultaneously accounting for the influence of T and S on the Raman band is connected with its complex nature, and it is possible to expect a substantial difference in the influence of temperature and admixtures on different components of the spectrum.

One of the first and important stages of Raman spectra processing was Fourier smoothing.[14] In our case, we used the 'unit' low-wavenumber Fourier filters, decreasing at the edges according to a Gaussian or Lorentzian law. The spectra obtained were normalized to the unit area. Subsequently, the shape of the water Raman band was described with the help of a set of parameters:

$$\chi_{ij} = I(\nu_i)/I(\nu_j) \tag{1}$$

where ν_i and ν_j are some characteristic points of the spectrum (Fig. 1) and $I(\nu_i)$ and $I(\nu_j)$ are the Raman intensities at the points i, $j = \{1, 2, 3\}$.

Expanding the two-parameter function $\chi_{ij}(T, S)$ in a Taylor series in the vicinity of some point (T_0, S_0), we obtain the following system of equations:

$$\Delta\chi_{32} = \chi_{32} - \chi_{32}|_{T_0,S_0} = (\partial\chi_{32}/\partial T)|_{T_0,S_0}\Delta T + (\partial\chi_{32}/\partial S)|_{T_0,S_0}\Delta S + \ldots \tag{2}$$

$$\Delta\chi_{31} = \chi_{31} - \chi_{31}|_{T_0,S_0} = (\partial\chi_{31}/\partial T)|_{T_0,S_0}\Delta T + (\partial\chi_{31}/\partial S)|_{T_0,S_0}\Delta S + \ldots \tag{3}$$

Taking several terms and solving the system with respect to $\Delta T = T - T_0$ and to $\Delta S = S - S_0$, one can determine T and S of the water medium.

All the coefficients necessary to solve the system were obtained from experimental dependences $\chi_{ij}(T)$ and $\chi_{ij}(S)$ in the temperature range 20–80 °C and salinity range 5–35‰ ('normal' sea water diluted with the distillate).

The developed method for the simultaneous determination of temperature and salinity of sea water made it possible to measure these parameters in laboratory conditions with precisions of 0.7 °C and 1.0‰, respectively.[12,14]

This method was tested in natural conditions on the research vessel *Akademik Petrovsky*. Processing of the remote data for natural sea water with the 'three-wavenumber method' gave values of temperature and salinity that differed from the values of T and S measured by the contact method, on the average by 1.1 °C and 1.4‰, respectively.[14]

Such errors in the simultaneous determination of water characteristics do not satisfy the requirements of oceanology, hence the suggested method needed further development. The next variants of the method for the simultaneous determination of water temperature and salinity used the data on the Raman scattering signal, accumulated in all the spectral channels of the optical multi-channel analyzer used.

'Multi-wavenumber' method of simultaneous determination of water temperature and salinity from Raman spectra

Experimental investigations of temperature and concentration changes in the Raman spectra gave us reasons to assume a linear dependence of the Raman intensity on water temperature and salinity:

$$I_i = \alpha_{iT}T + \alpha_{iS}S + \gamma_i \tag{4}$$

where i is the number of the spectral channel of the optical multi-channel analyzer, α_{iT} and α_{iS} are coefficients that determine the influence of T and S on the water Raman spectrum in the ith channel, respectively, $\gamma_i = \beta_i + \nu_i$, where β_i is a constant bias, equal to the average Raman intensity in the ith channel at 0 °C and 0‰, and ν_i is the random error of signal measurement in the ith channel.

Under this assumption, the determination of T and S is a problem of least-squares minimization of the functional

$$Q = \sum_{i=1}^{N}(I_i - \alpha_{iT}T - \alpha_{iS}S - \gamma_i)^2 \tag{5}$$

where I_i is the intensity in the ith channel of the Raman spectrum of water with the sought parameters T and S.

Minimizing Q ($\partial Q/\partial T = 0$, $\partial Q/\partial S = 0$), we obtain the following system of equations:

$$\begin{cases} \sum_{i=1}^{N} I_i \alpha_{iT} - T \sum_{i=1}^{N} \alpha_{iT}^2 - S \sum_{i=1}^{N} \alpha_{iT}\alpha_{iS} - \sum_{i=1}^{N} \alpha_{iT}\gamma_i = 0 \\ \sum_{i=1}^{N} I_i \alpha_{iS} - T \sum_{i=1}^{N} \alpha_{iT}\alpha_{iS} - S \sum_{i=1}^{N} \alpha_{iS}^2 - \sum_{i=1}^{N} \alpha_{iS}\gamma_i = 0 \end{cases} \quad (6)$$

Solving this system of two equations, linear with respect to T and S, we obtain the values of T and S.

The average deviations of the values of water temperature and salinity, calculated with the help of the 'multi-wavenumber' method, from the values measured by the contact method in laboratory conditions were 0.4 °C and 0.5‰, respectively.

However, the 'multi-wavenumber' method of simultaneous determination of temperature and salinity of sea water also does not take into account several factors allowing us to improve the precision of T and S measurement, e.g. *a priori* information on the ranges of parameter changes, noise statistics, regularities in the change of the fluorescent pedestal that the Raman band sits on, etc. These factors are taken into account by the procedure based on the method of reduction.

Determination of water temperature and salinity from Raman spectra with the help of the method of reduction

The method of reduction[33] makes it possible to optimize the process of measurement and data processing with the purpose of minimizing the errors in determination of the chosen parameters of the object.

To measure the water temperature and salinity with the help of the method of reduction, the Raman spectra obtained were not smoothed, in order to preserve information about noise statistics. In this paper we shall not describe the reduction procedure itself, as it is a combination of complex mathematical operations and has been described elsewhere.[33] We shall only point out that the precision of parameter determination for this method turned out to be dependent on the amount of known *a priori* information. On average, the use of the method of reduction makes it possible to determine water parameters simultaneously with errors of about 0.4 °C and 0.4‰ in laboratory conditions and about 0.8 °C and 0.6‰ in natural conditions.

USE OF THE ANN METHOD FOR THE SOLUTION OF INVERSE PROBLEMS IN RAMAN SPECTROSCOPY OF WATER

In recent years, a widely used method of solution of inverse problems has been the method of artificial neural networks (ANN).[34] ANN are a powerful tool capable of solving different problems of pattern recognition, classification and prediction in situations when parallel testing of multiple hypotheses and high computational speed are required, and where the best existing computer systems are much less effective than the corresponding human systems.

The simplest node of the network, called a neuron, has several inputs and one output. The neuron performs weighted summation of the inputs, and then a non-linear transformation of the result. More complex nodes may perform integration over time or other operations more complex than simple summation.[34]

An ANN is determined by the topology of node connections, by the characteristics of the nodes and by the learning rules. The learning capability determines such a unique property of an ANN as generalization of the provided information, and revealing hidden relations. There are different types of ANN, e.g. the three-layer perceptron and the general regression neural network.

The first stage of work with ANN is its training on known examples (patterns). The estimation of the training quality is performed on a test set. The test set is created in such a way that its patterns do not coincide with the patterns of the training set. This is necessary in order to prevent the net from memorizing the noise and from 'overfit.'

In addition to the mean squared error of parameter restoration, a good criterion for the ANN quality estimation is the coefficient of multiple determination R^2, described by the equation

$$R^2 = 1 - \frac{\sum_i (y_i - \tilde{y}_i)}{\sum_i (y_i - \overline{y})} \quad (7)$$

where y_i is the true value, $\tilde{y}_i$ is the predicted value and $\overline{y}$ is the mean value of the determined parameter y_i.

The ANN method itself gives no algorithm of calculation of errors for the restored parameters; therefore, to estimate the precision of parameter restoration, separate production (examination) data sets with different noise levels should be used.

Hence, to use neural networks, one needs a training set, a test set and several production sets.

We had made sure of the efficiency of this technique, having used it to solve the inverse problems in the non-linear fluorimetry of complex organic compounds.[35]

We began to use ANN in the Raman spectroscopy of water for the simplest one-parametric problem, i.e. for the determination of water temperature. In the future we intend to expand the program, investigating inverse problems with two and three parameters.

In the first stage, we used general regression neural networks[36] to estimate the precision of temperature determination from water Raman spectra. This ANN architecture seemed the most appropriate one in our case, as it was capable of giving good results when trained on a small number of patterns. From experimental spectra of the Raman valence band obtained before, we formed three data sets for ANN training: the training set (99 spectra in the temperature range 20–80 °C), the test set (36 spectra in the same range) and the production set (17 spectra in the same range). Only the most informative central part of the spectra was used. No smoothing of the curves was performed, since neural networks are stable to noise, and they can recognize useful information against a noisy background, which is undoubtedly one of their advantages.

The calculations were made with the help of the software package NeuroShell 2 from Ward Systems Group.

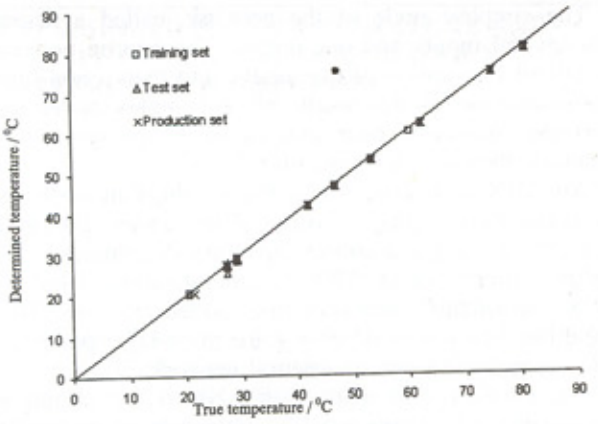

Figure 11. Scatter plot illustrating the determination of water temperature from the Raman spectra by means of ANN. Values on the abscissa correspond to true water temperatures and those on the ordinate to the temperatures predicted by ANN.

The results obtained are presented in Fig. 11 as a scatter plot, where the abscissa represents the true values of temperature and the ordinate the values determined by the neural network. It was determined that the relative mean squared error of temperature determination (on the production set) was about 0.4%, and the mean absolute error did not exceed 0.3 °C.

It is worth mentioning that the precision of temperature determination obtained from water Raman spectra with the help of artificial neural networks is better than the precision of temperature determination obtained by other methods.[14]

However, these results should be treated as preliminary, since the calculations used the available experimental data, that did not provide uniform filling of the whole desired temperature range. Therefore, in the future it is planned:

- to obtain new experimental Raman spectra of water, recorded frequently enough and uniformly over all of the desired range of temperature and salinity;
- to use new ANN architectures for the new experimental database;
- to apply ANN to the simultaneous determination of water temperature and salinity from the Raman spectra;
- to solve the three-parametric problem of diagnostics of the water medium, i.e. to determine the temperature, salinity and dispersion of the attenuation index (note that the first approach to such a task was made earlier[21] on the basis of the method of reduction);
- to verify the models of water structure by recognition of the 'images' of the water Raman band.

Acknowledgments

The authors express their gratitude to R. Yu. Orlov for the opportunity to use his equipment (autoclave), V. Shaporev for his help in conducting the experiments on it and the workers of the artificial intelligence laboratory of the Nuclear Physics Institute of Moscow State University for the opportunity to use the software package NeuroShell 2.

REFERENCES

1. Bunkin A, Pershin S. *Bull. Russ. Acad. Sci. Phys. Vibr.* 1997; **61**: 158.
2. Pershin S. Doctoral Thesis, Moscow State University, 1998.
3. Monosmith W, Walrafen G. *J. Chem. Phys.* 1984; **81**: 669.
4. Walrafen G, Hokmabadi M, Yang W. *J. Phys. Chem.* 1988; **29**: 2433.
5. Scherer J, Go M, Kint S. *J. Phys. Chem.* 1974; **78**: 1304.
6. Bansil R, Wiafe-Akenten J, Taafe I. *J. Chem. Phys.* 1981; **76**: 2221.
7. Yeh Y, Bilgram J, Kanzig W. *J. Chem. Phys.* 1982; **77**: 2317.
8. Leonard D, Chang C, Yang L. US Patent 3 986 775, 1974.
9. Leonard D, Caputo B, Hoge F. *Appl. Opt.* 1979; **18**: 1732.
10. Fadeev V. Doctoral Thesis, Moscow State University, 1983.
11. Bekkiev A, Fadeev V. *Sov. Phys. Dokl.* 1982; **27**: 63.
12. Bekkiev A, Gogolinskaya (Dolenko) T, Fadeev V. *Sov. Phys. Dokl.* 1983; **28**: 639.
13. Bekkiev A. PhD Thesis, Moscow State University, 1982.
14. Gogolinskaya (Dolenko) T. PhD Thesis, Moscow State University, 1987.
15. Panchishin I. PhD Thesis, Moscow State University, 1989.
16. Glushkov S, Panchishin I, Fadeev V. *Sov. j. Quantum Electron.* 1989; **16**: 843.
17. Kecki Z. *J. Mol. Struct.* 1992; **265**: 1.
18. Murphy W, Bernstein H. *J. Phys. Chem.* 1972; **76**: 1147.
19. Scherer J, Snyder R. *J. Chem. Phys.* 1977; **67**: 4794.
20. Glushkov S, Panchishin I, Fadeev V. *Sov. Phys. Dokl.* 1986; **31**: 982.
21. Patsaeva S. PhD Thesis, Moscow State University, 1989.
22. Iwata T, Koshoubu J, Chihiro J, Okubo Y. *Appl. Spectrosc.* 1997; **51**: 1269.
23. Schiffer J, Hornig D. *J. Chem. Phys.* 1968; **49**: 4150.
24. Efimov Yu, Naberuhin Yu. *Zh. Strukt. Khim.* 1980; **21**: 95.
25. Gorbatyi Yu, Dem'yanec Yu. *Zh. Strukt. Khim.* 1980; **21**: 76.
26. Kalinichev A, Bass J. *J. Phys. Chem. A* 1997; **101**: 9720.
27. Postorino P, Tromp R, Ricci M-A, Soper A, Neilson G. *Nature (London)* 1993; **366**: 668.
28. Scheeltz G, Hornig D. *J. Phys. Chem.* 1961; **65**: 2131.
29. Abe N, Ito M. *J. Raman Spectrosc.* 1978; **7**: 161.
30. Goncharov V, Romanova I, Samoilov O, Yashkichev V. *Zh. Strukt. Khim.* 1967; **8**: 613.
31. Klyshko D, Fadeev V. *Sov. Phys. Dokl.* 1978; **23**: 55.
32. Fadeev V. In *Abstracts of the 1st Conf. on Luminescence*, Czeged, Hungary, 1976; 7.
33. Pyt'ev Yu. *Russ. Math. Sb.* 1983; **1**(5): 19.
34. Lippman R. *IEEE ASSP Mag.* 1987; **3**: 4.
35. Fadeev V, Dolenko T, Filippova E, Chubarov V. *Opt. Commun.* 1999; **166**: 25.
36. Specht D. *IEEE Trans. Neural Networks* 1991; **2**: 568.